International Atomic Energy Agency

INDC(GDR)-17/L

INDC INTERNATIONAL NUCLEAR DATA COMMITTEE

The High-Energetic Part of the Cf-252 Spontaneous-Fission Neutron Spectrum

H. Maerten, D. Seeliger and B. Stobinski
Technical University Dresden, GDR

May 1982

IAEA NUCLEAR DATA SECTION, WAGRAMERSTRASSE 5, A-1400 VIENNA

Reproduced by the IAEA in Austria
May 1982

THE HIGH-ENERGETIC PART OF THE CF-252 SPONTANEOUS-FISSION NEUTRON SPECTRUM

H. Märten, D. Seeliger and B. Stobinski

Technical University Dresden, GDR

January 1982

Abstract

Employing a high-sensitive neutron spectrometer based on the electronic n/γ,μ-discrimination and the two-dimensional measurement of neutron time-of-flight (TOF) and scintillator proton recoil energy (PRE) the high-energetic part of the Cf-252(sf) neutron spectrum was determined up to 28 MeV. Within the experimental errors, the resulting spectrum agrees with the corresponding NBS evaluation up to 16 MeV, whereas it is strongly superelevated above 20 MeV with reference to the Maxwellian distribution with kT = 1,42 MeV.

1. Introduction

Properly fission neutron spectra extend to relatively high energies. Considering the energy balance in fission, on principle, energies up to about 40 MeV are possible. Because of the very low emission cross sections in the high-energy range fission neutron spectra are measurable up to about 15 MeV commonly. The physical interest in this matter stimulated our effort to determine the high-energy end of fission neutron spectra experimentally /6,7/.

The importance of such measurements is confirmed in the case of the neutron emission spectrum from the spontaneous fission of Cf-252, because it was recommended as a standard /1/. Hitherto, its validity at high emission energies is not determined exactly due to the high measurement errors above 10 MeV. Data of different authors diverge substantially /2/. The result of the NBS evaluation /3/ was stated by a correction function $\mu(E)$ with reference to the Maxwellian distribution with kT = 1,42 MeV:

$$N(E) = \mu(E) \cdot 0{,}6672 \cdot E^{1/2} \cdot \exp(-E/1{,}42) \qquad (1)$$

(see table 1). Some recent measurements /4/ and evaluations /5/ are consistent with that of Grundl and Eisenhauer (NBS) /3/.

2. Experimental arrangement

As described in ref. 8 in more detail, the high sensitivity of the neutron spectrometer is based - besides the use of a high-efficient neutron detector with a voluminous NE 213 scintillator (5'' thick, 5'' diameter) - on the heavy shielding and the electronic $n/\gamma,\mu$-discrimination to reduce the experiment-specific and the cosmic background as well as on the two-dimensional (TOF,PRE)-measurement.

The electronic system for particle discrimination by the charge comparison method is used to suppress the background counts of the detector caused by γ-rays and penetrating components of the cosmic rays. Especially cosmic myons with energies around 1 GeV give rise to a background part with about 3,5 s^{-1} event rate and an average pulse height of about 25 MeV with reference to PRE (fig. 2b). The n/μ-discrimination method enables the suppression of the cosmic background to less than 0,5 % in the region of the myon hump of the pulse height background spectrum.

Measuring neutron TOF and PRE two-dimensionally one is able to select the optimum (regarding background conditions) PRE range for a given TOF channel or channel range in the analysis, which is carried out cyclicly in connection with PRE interval variation. Two analogous-to-digital converters, which recieve the time-to-analogous converter output and the PRE spectroscopic pulse, work in coincidence with the neutron identifying output signal of the electronic particle discrimination system. The derived 12 bit sum words (64 channels x 64 channels) are stored in an intermediate memory of 4 K capacity, which represents - in connection with a display unit - a multi-channel analyser (fig. 1). The experiment aimed at the measurement of the high-energetic part of the Cf-252(sf) neutron spectrum was practicable measuring a limited TOF range, which was required because of the relatively small TOF channel interval.

The spectrometer is coupled to a minicomputer, which arranges the control of the two-dimensionally working multi-channel analyser for data acquisition, the check (regarding TOF peak and PRE edge positions) and correction of the spectra as well as their analysis. The corresponding program system was elaborated by the use of the high-level language FORTRAN 4000/4200 including CAMAC and display application subroutines /9/.

The zero-time signal is obtained employing a fast ionisation fission chamber /10/ for direct fragment detection. It is characterized by a very light construction. The fission event rate amounted to $3{,}40 \cdot 10^4\ s^{-1}$ at the beginning of the measurement. The Cf-252 sample has to be located in the axis of the collimating system (shielding) at a distance L (the path of flight) from the scintillator centre in such a manner, that this axis stands perpendicular to the electrode plane. In this way, systematic errors due to the anisotropic fragment detection are avoided widely.

The whole time resolution of the described arrangement amounts to 1,8 ns regarding FWHM of the γ-peak. It is somewhat higher for neutrons due to the dimension of the scintillator and, hence, neutron energy dependent. To guarantee a sufficiently good energy resolution for high neutron energies a relatively high path of flight is required ($L \gtrsim 4$ m).

The calibration of the two-dimensional spectrum coordinates is realized in the following manner:

i) The calibration of the time coordinate is carried out by additional measurements using a defined delay device (Δt = (96,97 $\pm$ 0,30) ns) and considering the γ-peak as a fixed TOF point.

ii) The PRE edge position (point of inflexion) for a given TOF channel or neutron energy EN corresponds to EN but a systematic deviation because of the distortion of the PRE response function by multiple detection processes. This effect was studied using the Monte Carlo code NEUCEF /11/ after determining an effective parameter which characterizes the finite pulse height resolution of the detector by a fit of calculated to experimental PRE response functions. Considering the corresponding correction factor (2 to 8 %), which was obtained with an error of about 20 %, the calibration of the PRE coordinate is possible by the use of the measured continuous spectrum itselfes due to the energy selection by TOF measurement. The accuracy of this calibration method depends on statistics and channel resolution mainly /6,9/.

Generally the background is a function of TOF. This effect doesn't appear at sufficiently high PRE. Therefore, it is possible to reduce the common conception of the alternating measurements with and without sample on the sole measurement with sample. The background is determined from a defined region of the (TOF,PRE)-plane, where no effect events appear for physical reasons.

3. Detector efficiency

First of all, the detector efficiency was calculated by the use of the Monte Carlo code NEUCEF /11/ accepting the light output data of Verbinski et al. /12/ and real values of the mentioned pulse height resolution parameter and geometric factors.
An efficiency matrix as a function of EN and PRE threshold was built on the basis of the calculated data.

A first measurement of the Cf-252(sf) neutron spectrum, which is known with an uncertainty of less than 2,5 % between about 0,4 and 7 MeV /5/, was aimed at the comparison of the calculated with the measured efficiency data for relatively high threshold energies. We assumed the NBS evaluated spectrum for efficiency determination. The measurement was carried out on the basis of 4,0 m path of flight and during a whole measuring time of 62,0 h. Typical TOF spectra for different PRE thresholds are shown in fig. 4. The corresponding normalized energy spectra, which were determined presuming the calculated efficiency data,

can be seen in fig. 5 compared with the NBS spectrum. Both spectra agree well. Hence, the efficiency functions, which were determined for different threshold energies on the basis of the NBS evaluated spectrum, confirm the NEUCEF data absolutely within an error which is EN and PRE threshold dependent.
It amounts to about 5 % in the ranges of best statistics.
It is amphazised that the description of the experimental efficiency data by the NEUCEF code is rather good in the threshold region due to the consideration of resolution effects (fig. 6).

4. Characterization of the experiment

The long-time experiment (1218,5 h whole measuring time) was carried out on the same conditions as the measurement aimed at the confirmation of the efficiency data in the MeV region excepting the path of flight, which was decided to be somewhat longer (4,5 m). The measurement could be subdivided in only five runs because of the relatively good stability of the spectrometer. Timing drifts were lower than 400 ps during the whole measurement time. This effect was corrected.
PRE edge positions in the MeV region didn't change within an uncertainty of about 150 keV (with reference to PRE).

The performance of the particle discrimination system was checked by the use of the oscillograph method (fig. 1) continuously. Small variations of the particle discriminator threshold were corrected. Nevertheless, the found optimum

PRE ranges for the analysis of the high-energy spectrum part were somewhat different for the single runs (table 2). Therefore, the single spectra were analysed seperately and thereupon concentrated considering weight factors because of the different run times.

The TOF spectrum of the whole measurement, which was determined for the limited PRE range from 9,44 to 16,64 MeV, is shown in fig. 7. The effect TOF distribution extends to about 28 MeV. The background level per TOF unit, PRE unit and measuring time respectively was found to be smaller than $1{,}5 \cdot 10^{-4}$ ns^{-1} MeV^{-1} h^{-1} in the used PRE ranges. This value illustrates the sensibility of the experiment.

The summarized energy distribution was corrected for time resolution, which affects the measured spectrum in the high-energy part especially, and for the influence of the TOF channel width, which was relatively high (2,372 ns) due to the limited storage capacity /9/. Dead-time corrections were neglegible because of the low event rate ($\sim 5\ s^{-1}$).

The ultimate energy spectrum is listed in table 3 and illustrated in fig. 8 including the statistical error values, which were determined on the basis of the Student t distribution (75 % certainty).

Accepting the measurement described in paragraph 3 as a test of measurement accuracy and considering the higher uncertainty of efficiency calculation for higher neutron energies the following measurement errors (excepting the statistical one) are assumed for the experimental determination (carried out absolutely) of the high-energy end of the Cf-252(sf) neutron spectrum: 8 % for the emission energy range from 10 to 15 MeV, 12 % from 15 to 20 MeV and 15 % above 20 MeV.

5. Concluding remarks

Fig. 9 represents the percentage departure of our data from the Maxwellian distribution with kT = 1,42 MeV in comparison with the results of some other groups as well as with the NBS evaluated spectrum (fig. from ref. 2, supplemented). It illustrates the discrepancies of the results determined by different authors in the emission energy range above 8 MeV.

Our results are consistent with the NBS evaluation up to 16 MeV. The measured spectrum shows a shoulder-like structure above 20 MeV. The corresponding neutron yield is much higher as expected:

$$\int_{E_1}^{E_2} N(E)\,dE = (9{,}8 \pm 5{,}3) \cdot 10^{-6} \text{ for } (20{,}1;26{,}7),$$
$$(6{,}0 \pm 3{,}4) \cdot 10^{-6} \text{ for } (21{,}5;26{,}7),$$
$$(5{,}1 \pm 3{,}0) \cdot 10^{-6} \text{ for } (23{,}2;26{,}7)$$

(error with reference to 90 % certainty).

Furtheron, the high-energy end of the measured spectrum is not describable in the framework of a detailed cascade-evaporation model (fig. 8). It was applicated considering realistic initial excitation energy distributions as a function of fragment mass number /6/, i. e. other emission mechanisms are prevalent in formation the high-energy part of fission neutron spectra /6,7/.

The changing slope of the spectrum in the energy range from 20 to 25 MeV was found in four of the five independent measuring runs. This fact is one argument against the possibility of equipment effects as the reason of the measured spectrum shape. On the other hand, the measured effect also appears at higher PRE thresholds, but the statistical errors become higher.

Our experimental results on the high-energy end of the neutron spectrum from the spontaneous fission of Cf-252 may be summarized as follows:

i) Within the experimental errors, the NBS evaluated spectrum was confirmed up to 20 MeV (in a qualified sense for the range from 16 to 20 MeV).

ii) For the energy interval from 20 to 28 MeV the correction function

$$\mu(E) = \exp(+\ 0{,}65 \cdot (E - 20{,}65)) \qquad (2)$$

with reference to the Maxwellian distribution with $kT = 1{,}42$ MeV (equ. 1) was determined.

Acknowledgements

The authors gratefully acknowledge the help of W. Grimm and R. Krause in the minicomputer and CAMAC application.

References

/1/ Report INDC-36/LN, INDC/NEANDC, Nuclear Standards File, 1980 version, p. B-38.

/2/ M. V. Blinov, Proc. IAEA Consultants Meeting on Neutron Source Properties, INDC(NDS)-114/GT (1980).

/3/ J. Grundl and C. Eisenhauer, Natl. Bur. Stds. Pub., NBS-493 (1977).

/4/ J. Boldeman, Trans. Am. Nucl. Soc., 32, 733 (1979).

/5/ B. I. Starostov et al., Jad. Konst. 2(37), 3 (1980).

/6/ H. Märten, Thesis, Technical University Dresden (1980).

/7/ H. Märten and D. Seeliger, Proc. Int. Symp. on Special Topics of the Interaction of Fast Neutrons and Heavy Ions with Atomic Nuclei, Gaußig (1980), ZfK-report (1981).

/8/ W. Grimm, H. Märten and D. Seeliger, Proc. Conf. on Neutron Physics, Kiew (1980), Vol. III, p. 3.

/9/ W. Grimm, H. Märten, D. Seeliger and B. Stobinski, Proc. Int. Conf. on the Interaction of Fast Neutrons with Nuclei, Rathen (1981), ZfK-report (1982), to be published.

/10/ M. Adel-Fawzy et al., Kernenergie 24, 107 (1981).

/11/ N. R. Stanton, COO-1545-92 (1971),
D. Hermsdorf, ZfK-315, 192 (1977).

/12/ V. V. Verbinski et al., Nucl. Instr. Meth. 65, 8 (1968).

/13/ Z. A. Alexandrova et al., Atomnaya Energiya 36, 282 (1974).

/14/ N. N. Knitter et al., Atomkernenergie 22, 84 (1973).

/15/ H. Werle and H. Bluhm, Prompt Fission Neutron Spectra (Proc. Consult. Meeting, Vienna, 1971), IAEA, Vienna (1972), p. 65.

Table 1

The correction functions $\mu(E)$ according to equ. 1

$\mu(E)$	Energy range	Reference
$1 + 1{,}20 \cdot E - 0{,}237$	0,0 - 0,25	/3/
$1 - 0{,}14 \cdot E + 0{,}098$	0,25 - 0,8	/3/
$1 + 0{,}024 \cdot E - 0{,}0332$	0,8 - 1,5	/3/
$1 - 0{,}0006 \cdot E + 0{,}0037$	1,5 - 6,0	/3/
$\exp(- 0{,}03 \cdot (E - 6{,}0))$	6,0 - 20	/3/
$\exp(+ 0{,}65 \cdot (E - 20{,}65))$	20 - 28	this work

Table 2

Measuring times and optimum PRE ranges (B_1,B_2) of the single runs

Run number	Time/h	B_1/MeV	B_2/MeV
1	210,0	7,16	19,67
2	495,0	9,06	18,54
3	98,5	9,44	17,40
4	245,0	9,82	21,57
5	170,0	6,78	21,57

Table 3

The high-energy end of the neutron spectrum from the spontaneous fission of Cf-252 (ultimate results) and the corresponding statistical errors (75 % certainty)

E/MeV	$N(E)/MeV^{-1}$	N/MeV^{-1}
11,1	$7,66 \cdot 10^{-4}$	$0,33 \cdot 10^{-4}$
11,7	$5,18 \cdot 10^{-4}$	$0,40 \cdot 10^{-4}$
12,3	$3,33 \cdot 10^{-4}$	$0,13 \cdot 10^{-4}$
12,9	$2,15 \cdot 10^{-4}$	$0,09 \cdot 10^{-4}$
13,6	$1,32 \cdot 10^{-4}$	$0,08 \cdot 10^{-4}$
14,4	$8,26 \cdot 10^{-5}$	$0,84 \cdot 10^{-5}$
15,3	$4,26 \cdot 10^{-5}$	$0,61 \cdot 10^{-5}$
16,2	$2,51 \cdot 10^{-5}$	$0,34 \cdot 10^{-5}$
17,2	$1,51 \cdot 10^{-5}$	$0,23 \cdot 10^{-5}$
18,3	$6,87 \cdot 10^{-6}$	$3,80 \cdot 10^{-6}$
19,5	$2,21 \cdot 10^{-6}$	$2,10 \cdot 10^{-6}$
20,8	$2,03 \cdot 10^{-6}$	$1,54 \cdot 10^{-6}$
22,3	$1,10 \cdot 10^{-6}$	$0,80 \cdot 10^{-6}$
24,0	$1,59 \cdot 10^{-6}$	$1,00 \cdot 10^{-6}$
25,8	$1,31 \cdot 10^{-6}$	$1,20 \cdot 10^{-6}$
27,9	$1,30 \cdot 10^{-6}$	$1,20 \cdot 10^{-6}$
30,2	$4,10 \cdot 10^{-7}$	$9,40 \cdot 10^{-7}$

Figures

Fig. 1

Schematic representation of the spectrometer and its on-line coupling to the minicomputer (C - control unit; O/I - output/input device; AS - interface device; AS 10 - CAMAC interface unit; DMA - direct memory access; SP - serial plotter; PTP/PTR - paper-tape puncher/reader).

Fig. 2a

Two-dimensional representation of the performance of the particle discrimination system (K_p - channel number, particle spectroscopic pulse; K_E - channel number, energy spectroscopic pulse; p, e, μ - particle branches of recoil protons, Compton electrons and cosmic myons respectively). The weak lines indicate the 5 % level of the peak height for a given K_E.

Fig. 2b

Pulse height spectrum of cosmic myons deduced from the measurement illustrated in fig. 2a (KI - counts per channel).

Fig. 3

Illustration of the two-dimensional (TOF,PRE)-measurement in the case of a 14,5 MeV neutron peak in connection with the corresponding one-dimensional spectra (neutron TOF spectra for different PRE thresholds; PRE spectrum and its differentiated form). On principle, the effect counts appear below the curve which represents the maximum PRE for a given TOF channel or neutron energy.

Fig. 4

Typical neutron TOF spectra for different PRE thresholds (parameter in MeV) from the spontaneous fission of Cf-252 deduced from the two-dimensionally measured spectrum in the analysis (4,0 m path of flight; 62,0 h measuring time; KI - counts per channel; K_t - TOF channel number; E - neutron energy).

Fig. 5

Neutron energy spectra, which correspond to the TOF spectra represented in fig. 4, determined presuming calculated detector efficiency data (NEUCEF code). The lines show the NBS evaluated spectrum.

Fig. 6

Detector efficiency for different PRE thresholds (parameter in MeV). The lines represent the data calculated by the use of the NEUCEF code. The experimental values were obtained from the two-dimensional (TOF,PRE)-measurement of the Cf-252(sf) neutron spectrum (fig. 4) presuming the results of the NBS evaluation. The deviations in the case of the 3,76 MeV threshold energy are caused by the higher uncertainty of the PRE calibration due to the limited channel resolution. The errors are statistical ones.

Fig. 7

TOF spectrum of the whole measurement of the neutron energy distribution from the spontaneous fission of Cf-252 determined for the limited PRE range from 9,44 to 16,64 MeV.

Fig. 8

The high-energy end of the Cf-252(sf) neutron spectrum compared with the NBS evaluated spectrum (continuous line) and the result of a detailed cascade-evaporation calculation (dashed line).

Fig. 9

Percentage departure of our data (o - 1st experiment with 62,0 h measuring time; ● - 2nd experiment with 1218,5 h measuring time) from the Maxwellian distribution with kT = 1,42 MeV in comparison with the results of some other groups (representation from ref. 2; + - /4/; x - /13/; △▼- /14/; □ - /15/) as well as with the NBS evaluated spectrum.

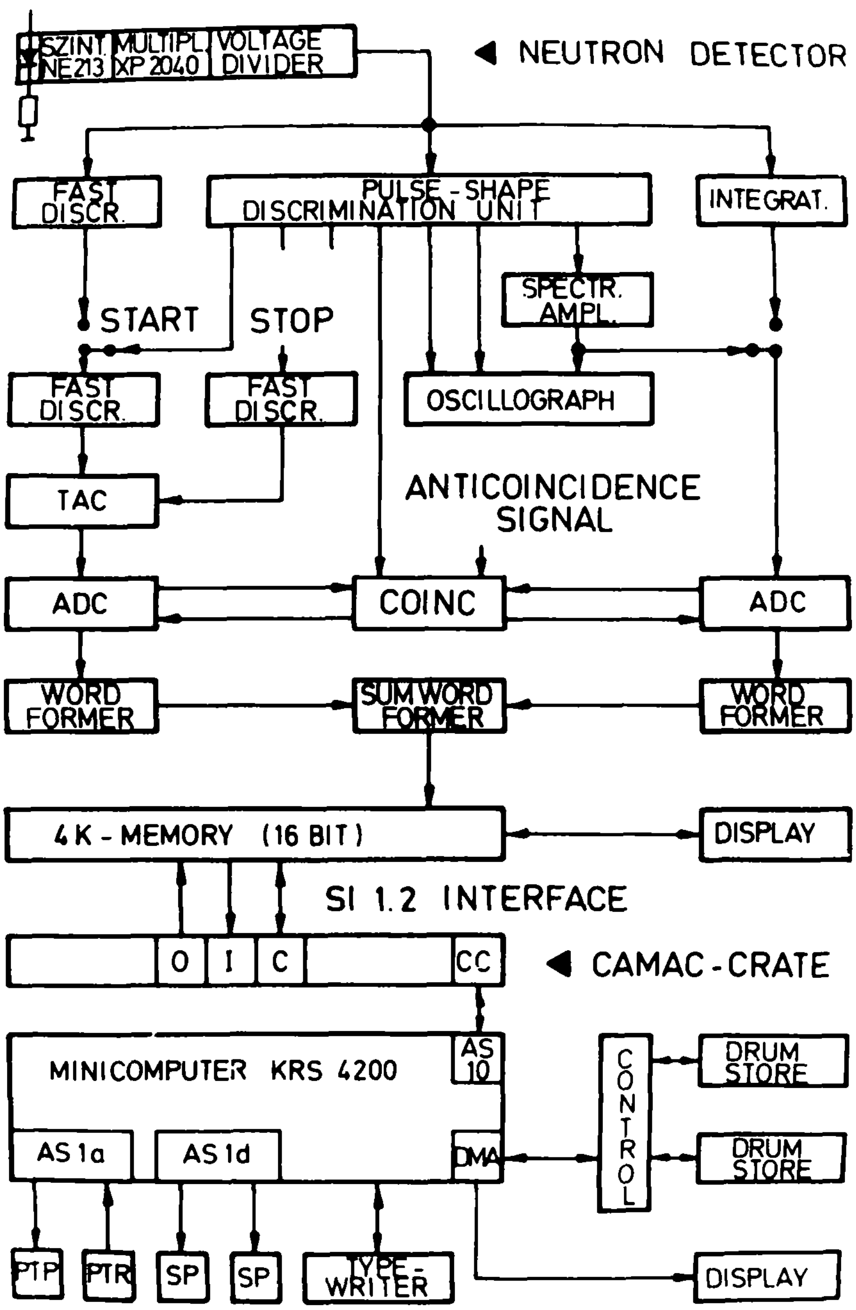
SZINT. NE213
MULTIPL. XP 2040
VOLTAGE DIVIDER
NEUTRON DETECTOR
FAST DISCR.
PULSE - SHAPE DISCRIMINATION UNIT
INTEGRAT.
SPECTR. AMPL.
START
STOP
FAST DISCR.
FAST DISCR.
OSCILLOGRAPH
TAC
ANTICOINCIDENCE SIGNAL
ADC
COINC
ADC
WORD FORMER
SUM WORD FORMER
WORD FORMER
4 K - MEMORY (16 BIT)
DISPLAY
SI 1.2 INTERFACE
O
I
C
CC
CAMAC - CRATE
MINICOMPUTER KRS 4200
AS 10
AS 1a
AS 1d
DMA
CONTROL
DRUM STORE
DRUM STORE
PTP
PTR
SP
SP
TYPE - WRITER
DISPLAY

Fig. 1

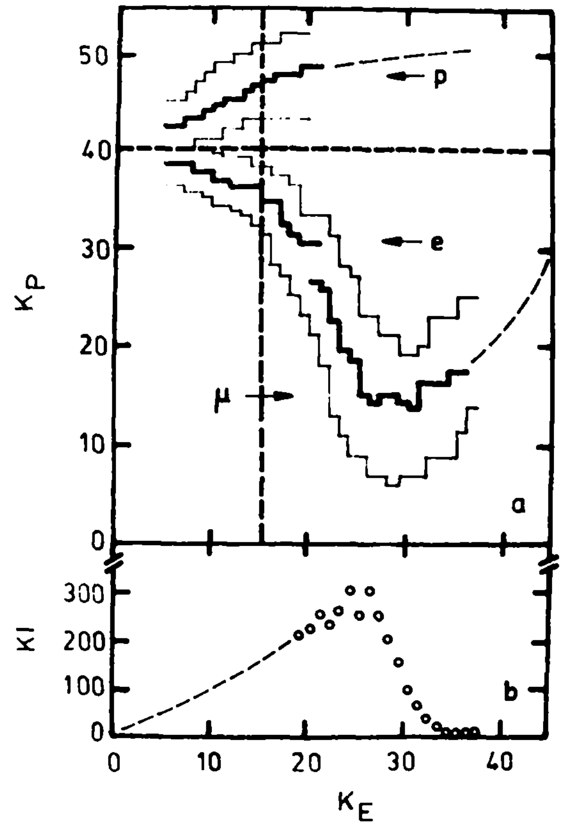

50
40
30
20
10
0
K_P
p
e
μ
a
300
200
100
0
KI
b
0
10
20
30
40
K_E

Fig. 2

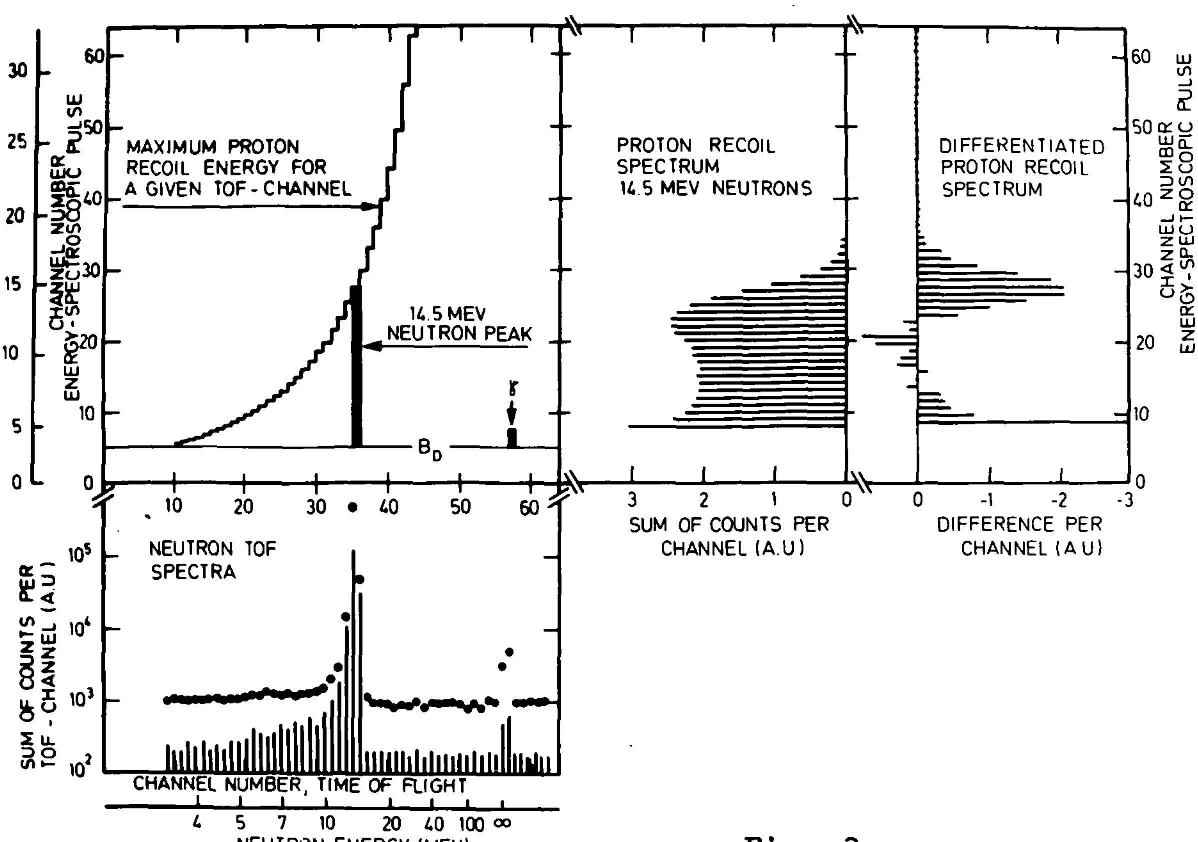

MAXIMUM PROTON RECOIL ENERGY FOR A GIVEN TOF-CHANNEL
14.5 MEV NEUTRON PEAK
γ
B_D
CHANNEL NUMBER ENERGY-SPECTROSCOPIC PULSE
PROTON RECOIL SPECTRUM 14.5 MEV NEUTRONS
DIFFERENTIATED PROTON RECOIL SPECTRUM
SUM OF COUNTS PER CHANNEL (A.U)
DIFFERENCE PER CHANNEL (A.U)
NEUTRON TOF SPECTRA
SUM OF COUNTS PER TOF-CHANNEL (A.U)
CHANNEL NUMBER, TIME OF FLIGHT
NEUTRON ENERGY (MEV)

Fig. 3

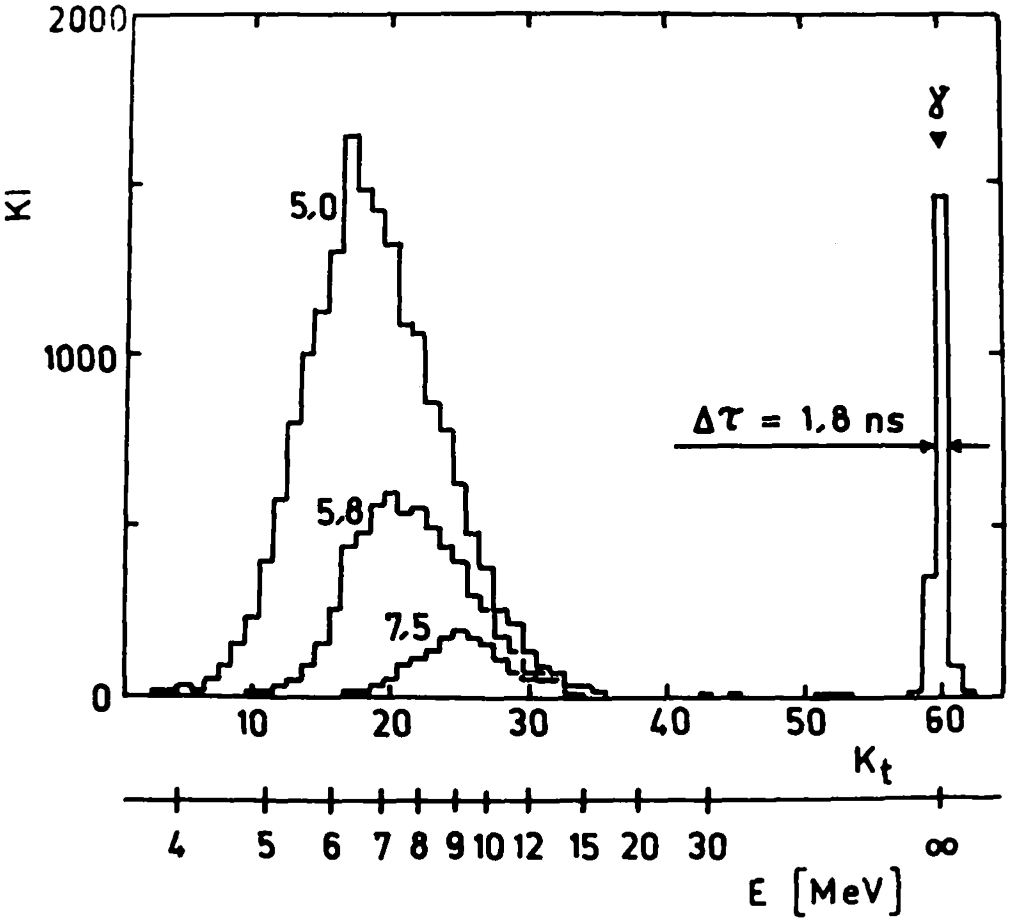
2000
1000
0
Kl
5,0
5,8
7,5
γ
Δτ = 1,8 ns
10 20 30 40 50 60
K_t
4 5 6 7 8 9 10 12 15 20 30 ∞
E [MeV]

Fig. 4

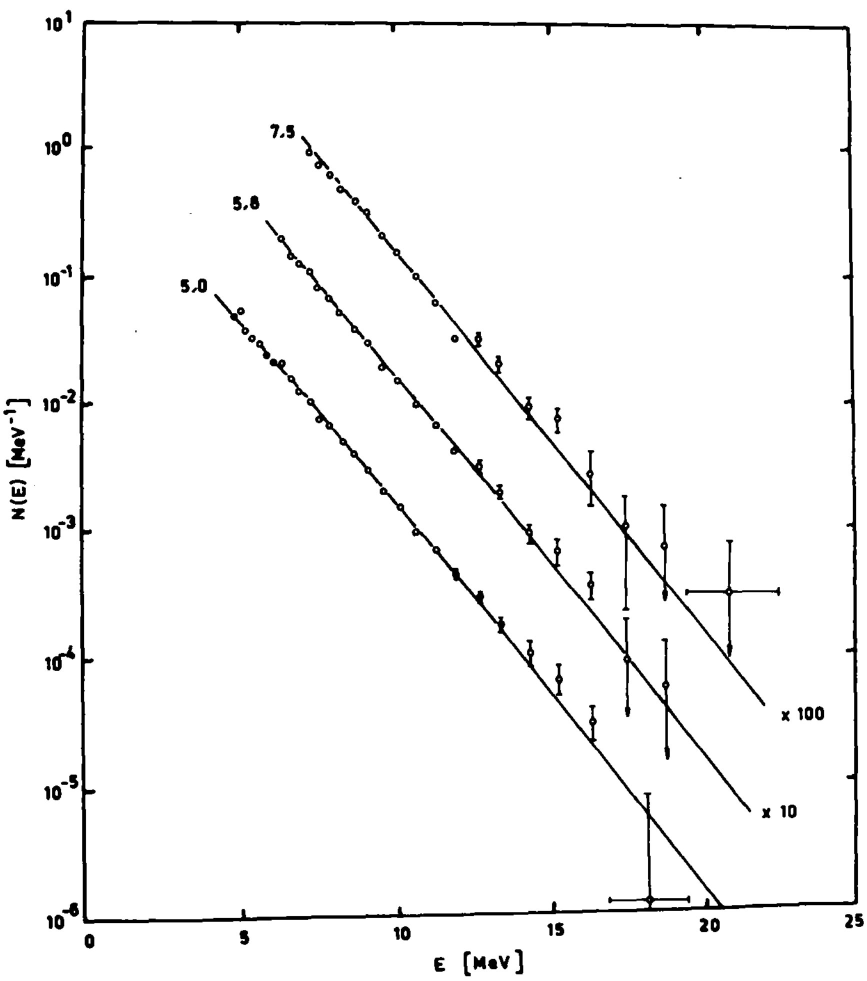
7.5
5.8
5.0
x 100
x 10
N(E) [MeV⁻¹]
E [MeV]
0 5 10 15 20 25

Fig. 5

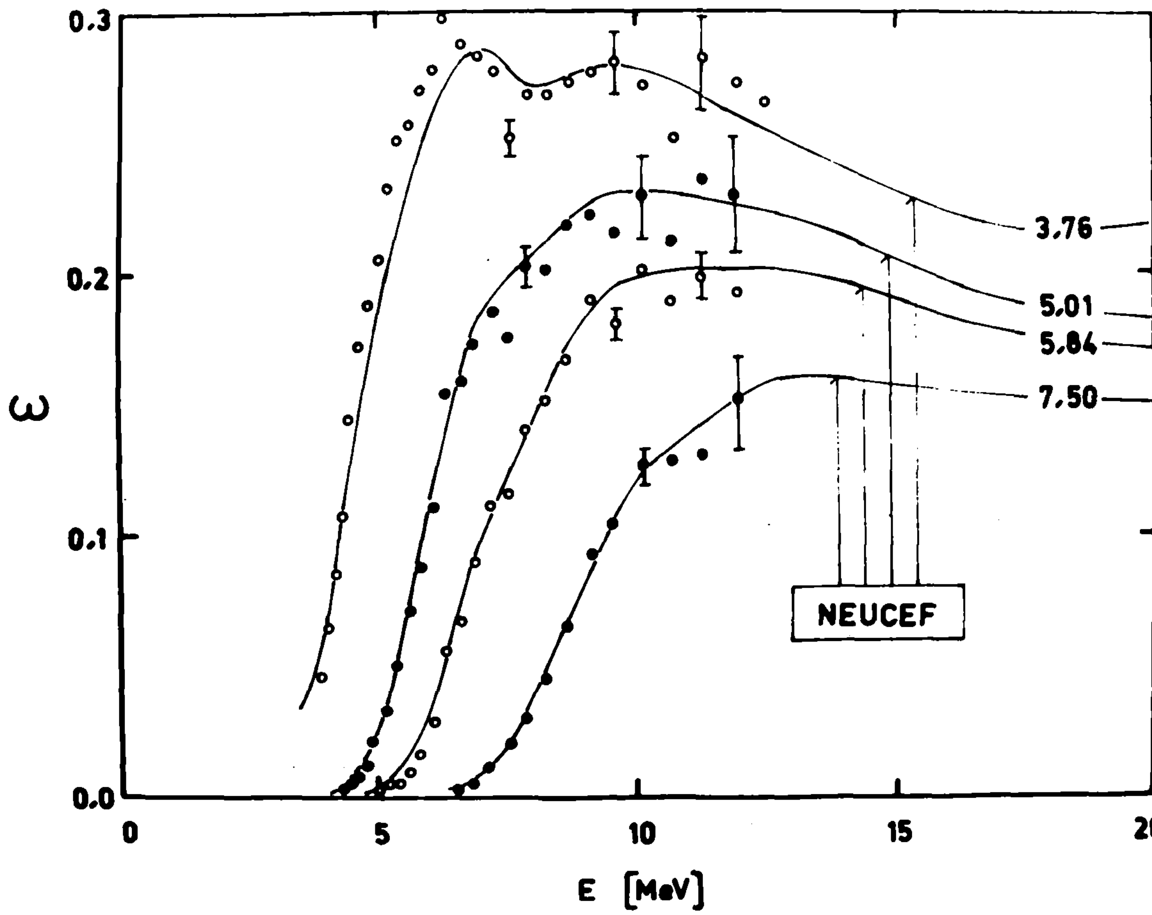

0.3
0.2
0.1
0.0
ω
0
5
10
15
20
E [MeV]
3,76
5,01
5,84
7,50
NEUCEF

Fig. 6

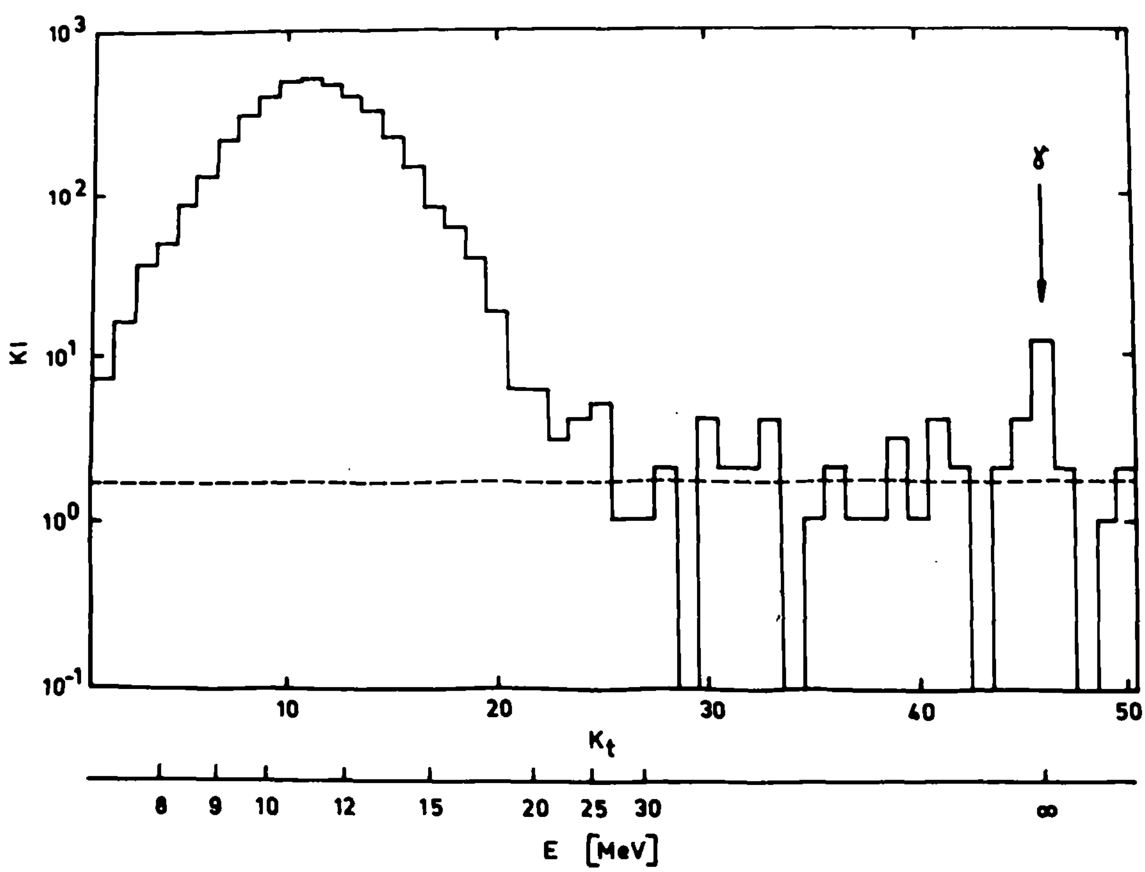

10³
10²
10¹
10⁰
10⁻¹
Kl
γ
10
20
30
40
50
K_t
8
9
10
12
15
20
25
30
∞
E [MeV]

Fig. 7

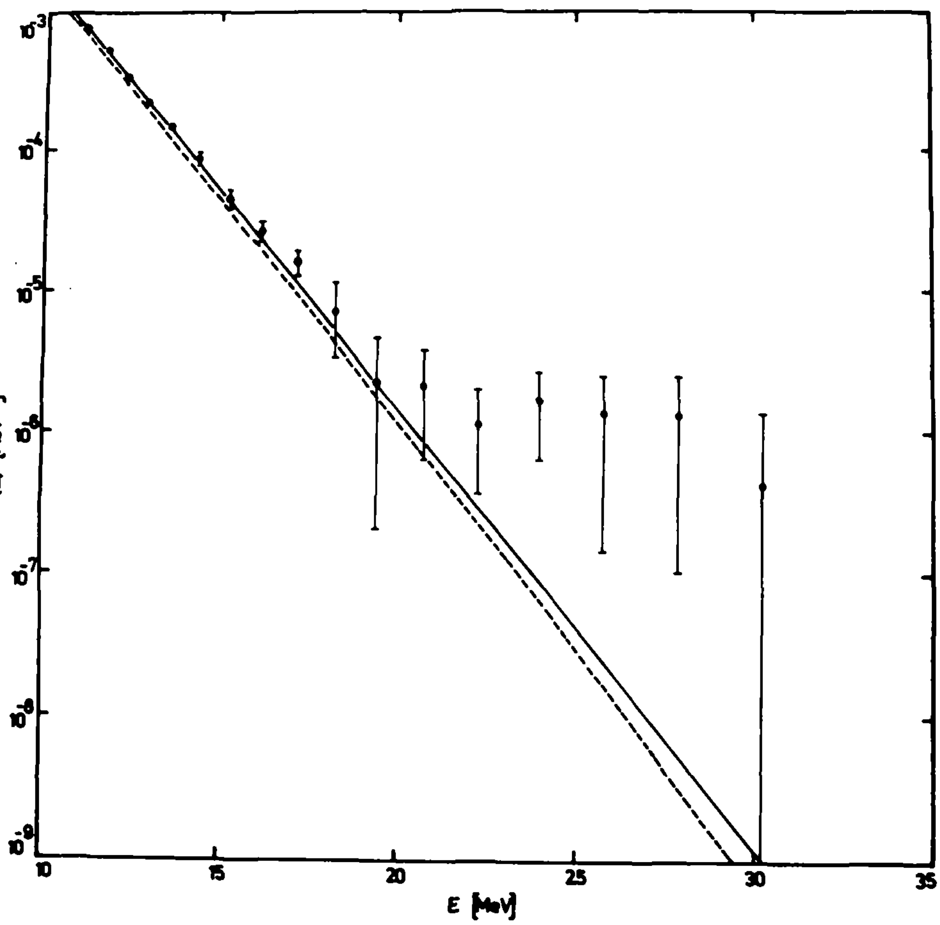
N(E) [MeV^{-1}]
E [MeV]
10
15
20
25
30
35

Fig. 8

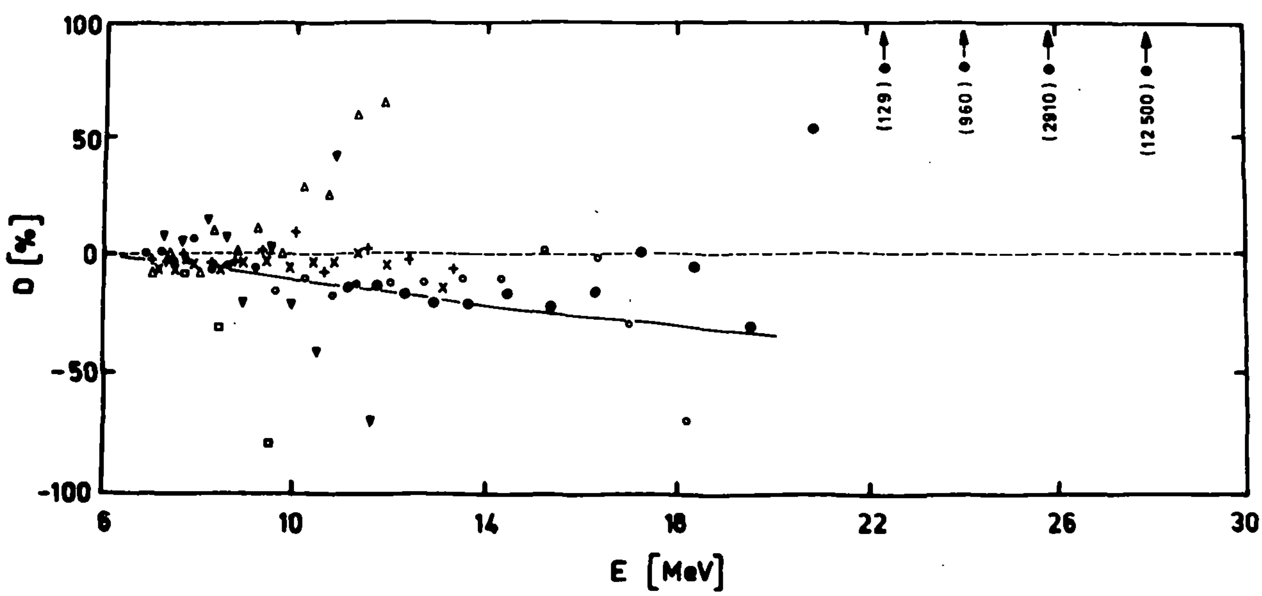
D [%]
E [MeV]
100
50
0
-50
-100
6
10
14
18
22
26
30
(129)
(960)
(2910)
(12 500)

Fig. 9